Computational Materials Science 173 (2020) 109407

Contents lists available at ScienceDirect

Computational Materials Science

journal homepage: www.elsevier.com/locate/commatsci

Competing effects of strain and vacancy defect on thermal conductivity of silicene: A computational study

M. Barati[a], T. Vazifehshenas[a,*], T. Salavati-fard[b,c], M. Farmanbar[d]

[a] Department of Physics, Shahid Beheshti University, G. C., Evin, Tehran 1983969411, Iran
[b] Department of Physics and Astronomy, University of Delaware, Newark, DE 19716, USA
[c] Department of Chemical and Biomolecular Engineering, University of Houston, Houston, TX 77204, USA
[d] Faculty of Science and Technology and MESA + Institute for Nanotechnology, University of Twente, P.O. Box 217, 7500 AE Enschede, The Netherlands

ARTICLE INFO

Keywords:
Lattice thermal conductivity
Silicene
Strain
Boltzmann transport equation
Vacancy defect

ABSTRACT

We theoretically investigate the thermal conductivity of freestanding silicene under isotropic tensile strain in a wide range of temperature and in the presence of important scatterings. Based on the phonon Boltzmann transport equation within the relaxation time approximation and using the strain-dependent force constants obtained from the first-principle calculations, we calculate the variations of thermal conductivity of strained infinite and finite-size silicene with the single-vacancy defects and boundary scatterings and compare them with those in the case of unstrained silicene. Particularly, we are interested in exploring the competition between the two opposing effects; strain induces enhancement and vacancy defects cause reduction in thermal conductivity. We show that the presence of vacancy defects has a more remarkable and much stronger effect in strained silicene and is able to remove or shift the peak created by strain in the thermal conductivity of infinite silicene. Interestingly, we find that the thermal conductivity suppression due to the vacancy defects varies with strain. Furthermore, presented results indicate that by increasing the temperature, the thermal conductivity becomes less sensitive to the strain and the difference between infinite and finite size samples gradually disappears. Finally, our calculations show that the effect of specularity parameter of boundary scattering is more pronounced at intermediate strain values.

1. Introduction

Since the discovery of graphene [1], two-dimensional (2D) materials have extensively been studied, owing to their unique and surprising physical and chemical properties as well as vast potential applications [2–13]. Silicene, a member of 2D materials family, having a buckled honeycomb lattice structure composed of Si atoms, exhibits exotic and particular characteristics [14–16]. Its buckled (rather than planar) structure breaks the inversion symmetry and produces intrinsic non-zero spin–orbit coupling interaction that opens up its energy bandgap [17,18]. The bandgap size can be controlled by applying an electric field. In addition, inequivalent Dirac points of silicene, which can be utilized by applying an exchange field, provide another degree of freedom for the carriers, i.e. valley [19,20]. On the other hand, the outstanding stretchability of 2D materials, allows direct tuning of their electrical, optical and thermal properties through strain engineering. For example, by applying an in-plane strain larger than 7.5% to silicene, a transition from semi-metal to metal is occurred [21]. These aspects and its compatibility with existing silicon-based technology, make silicene a promising material for nanoelectronics, valleytronics and thermoelectrics.

Despite extensive studies on the structural and electronic properties of silicene [3,5,22–33], its thermal transport characteristics are still open for further explorations. Although the high thermal conductivity is an appealing feature of a material for some applications such as electronic cooling and heat spreading [34,35], the thermoelectric applications demand materials with low thermal conductivity. Among various 2D materials, silicene with a small lattice thermal conductivity is an appropriate candidate for thermoelectrics.

To date, several theoretical studies using molecular dynamics (MD) and first principle-based solution of Boltzmann transport equation (BTE) have calculated the thermal conductivity of silicene [36–43]. Gu and Yang investigated the phonon transport in silicene and estimated a thermal conductivity of about 26 W/m.K at room temperature[36]. Using a modified Stillinger–Weber potential and anharmonic lattice dynamics (ALD) calculations, Zhang et al. found a thermal conductivity

* Corresponding author.
E-mail address: t-vazifeh@sbu.ac.ir (T. Vazifehshenas).

https://doi.org/10.1016/j.commatsci.2019.109407
Received 15 August 2019; Received in revised form 31 October 2019; Accepted 11 November 2019
Available online 21 November 2019
0927-0256/

smaller than 12 W/m.K while the ALD results (without Stillinger–Weber potential) predicted even smaller thermal conductivity [37]. In another computational study on the 2D group IV materials by Peng et al., a value of 28.3 W/m.K was obtained for the room-temperature thermal conductivity of silicene [38]. The effect of substrate on the thermal conductivity of silicene has also been reported in a few studies [41,42]. Wang et al. studied the thermal conductivity of free-standing and SiO_2 supported silicene by conducting MD simulations and concluded that the substrate leads to a 78% reduction in thermal conductivity at room temperature [41]. On the other hand, Zhang et al. realized that the thermal conductivity of silicene can be either enhanced or suppressed depending on substrate [42]. A review of some works on the thermal conductivity of silicene can be found in the first chapter of 'Silicene' [44]. The impacts of isotopic doping [45,46], boundary scattering [43] and vacancy defects [43,47] on phononic heat transfer have also been explored. In our previous work, we calculated the lattice thermal conductivity of unstrained silicene using BTE within the relaxation time approximation (RTA) and comprehensively investigated the effects of sample size, boundary scattering and single vacancy defects for a wide range of temperatures [43]. Our results indicated that the thermal conductivity of silicene is significantly suppressed by vacancy defects. We also showed that the phonon-boundary scattering is important in defectless and small-size silicene samples, specially at low temperatures.

The strain effects on the thermal conductivity of silicene have previously been investigated [39,40,45,48] and it was shown that small strain causes a significant increase in the thermal conductivity. Based on MD simulations, Pei et al. found that while small tensile strains lead to an increase in the thermal conductivity of silicene at room temperature, a reduction in thermal conductivity is achieved for strain values larger than 10% [45]. Hu et al. [48] predicted an anomalous thermal response to uniaxial tensile strain; first increases significantly with applied tensile strain and then fluctuates around some value. The first principles lattice dynamics calculations performed by Kuang et al. [40] showed that the tensile strains give rise to strong size effects for silicene thermal conductivity with a peak near 7% strain for large silicene samples. Xie et al. [39] computed the strain-dependent thermal conductivity of silicene under uniform biaxial tension at room temperature by solving the phonon BTE both in the RTA scheme and iteratively. They extracted the interatomic force constants from first-principles calculations for the strained silicene. Both RTA and iterative methods resulted in similar trends in the change of thermal conductivity with tensile strain. They found that the thermal conductivity of silicene which increases significantly with strain, has a clear dependency on the sample size so that it exhibits a peak at 4% strain for infinite silicene.

Motivated by the dramatic variations of silicene thermal conductivity with temperature, vacancy defects and strain, in this study, we consider silicene structure under uniform biaxial tensile strain (in this situation when strain becomes larger, the lattice constant is uniformly increasing) and examine both separate and combined effects of temperature, phonon-boundary and phonon-vacancy defect scatterings on the thermal conductivity. We are particularly interested in looking for the dominant effect on the thermal conductivity in strained silicene case. We employ the RTA method which has been successfully applied to the strained silicene [39] by using the strain-dependent harmonics and anharmonic force constants obtained from first-principles calculations.

This paper is organized as follows: in Section 2 the theory is given and the method is explained, briefly. In Section 3 the results are presented and discussed, in detail. Finally, findings of this work are summarized in Section 4.

2. Theory and method

We consider a free-standing monolayer silicene with an unstrained buckling of 0.45 Å. We assume that silicene is under an uniform biaxial tensile strain which decreases the buckling height (Fig. 1). Due to the small amount of electronic contribution to the thermal conductivity, we consider only the phononic part of the thermal conductivity of silicene. We use RTA solution of the phonon BTE to compute the thermal conductivity of free-standing monolayer silicene.

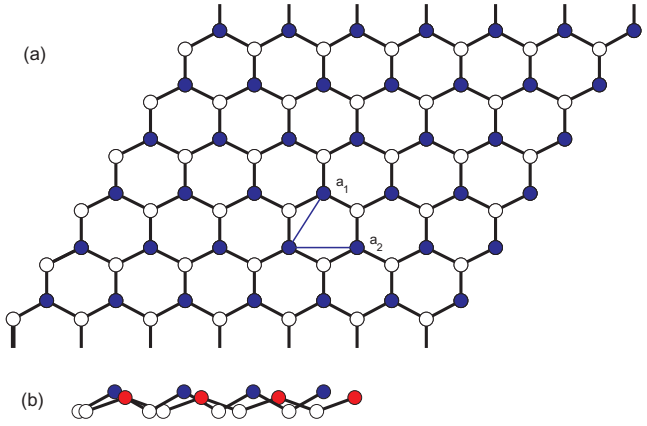

Fig. 1. (a) Top view of silicene in the x-y plane: $\boldsymbol{a_1}$ and $\boldsymbol{a_2}$ are the lattice vectors. (b) side view of unstrained (blue and white circles) and strained silicene (red and white circles) in the x-z plane.

The phonon thermal conductivity of silicene, κ, including contributions from of all phonon modes can be expressed as [43]:

$$\kappa = \frac{\hbar^2}{V k_B T^2} \sum_{\lambda} \omega_\lambda^2 v_\lambda^2 n_\lambda^0 (1 + n_\lambda^0) \tau_\lambda, \tag{1}$$

Here, $\hbar$, k_B, V, T, v_λ, n_λ^0 and τ_λ are the Plank constant divided by 2π, Boltzmann constant, volume of the unit cell, temperature, phonon velocity of mode λ ($\lambda = (\mathbf{q}, s)$, where $\mathbf{q}$ stands for the phonon wave vector and s denotes branch index), equilibrium distribution function and phonon lifetime, respectively. The phonon frequency, ω_λ, is obtained from the square root of the s-th eigenvalue of the dynamical matrix of the system, which its ($\alpha\beta$) Cartesian component, $D^{\alpha\beta}(\mathbf{q})$, is given by: [36,43]:

$$D_{jj'}^{\alpha\beta}(\mathbf{q}) = \frac{1}{\sqrt{M_j M_{j'}}} \sum_{\mathbf{R}'} \phi_{0j\mathbf{R}'j'}^{\alpha\beta} e^{i\mathbf{q}.\mathbf{R}'}, \tag{2}$$

where $\phi_{0j\mathbf{R}'j'}^{\alpha\beta}$ is the harmonic interatomic force constant. As it is expected, the changes of both harmonic and anharmonic interatomic force constants due to strain have an important effect on the thermal conductivity results. So, we use the strain-dependent harmonic interatomic force constants extracted from the first-principle calculations performed by Xie et al. [39] and obtain the phonon dispersion of monolayer silicene at some typical strains. It is worth pointing out that the correctness of phonon dispersion was verified by comparing our results with those reported in [39]. The dispersions of different phonon branches of 3% and 8% strained silicene are shown in Fig. 2 where ZA, TA and LA refer to the flexural or out-of-plane, transverse and longitudinal acoustic branches and ZO, TO and LO denote the flexural, transverse and longitudinal optical branches. For comparison, the results for the unstrained silicene are also displayed in this figure. The major changes due to the strain are shifting the optical modes downwards and making the acoustic branches closer to each other. These effects, as shown later, increase the contributions of these modes to the thermal conductivity through the strain-dependent phonon scattering processes.

The phonon lifetime, τ_λ, is expressed as [49,50]:

$$\tau_\lambda = \tau_\lambda^0 (1 + \Delta_\lambda). \tag{3}$$

In the above equation Δ_λ reflects the inelastic nature of three-phonon

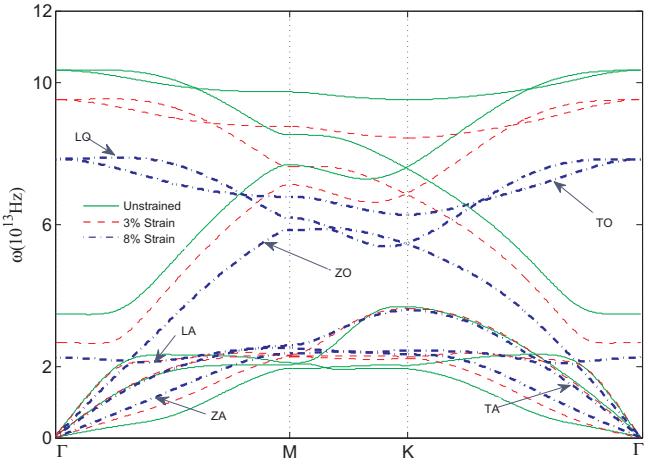

Fig. 2. Phonon dispersions of unstrained and strained silicene of 3% and 8% strains.

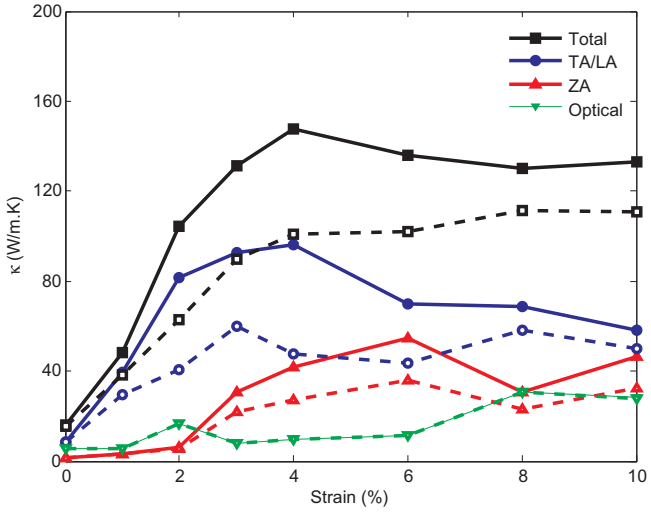

Fig. 3. Thermal conductivity of silicene and contributions from different branches as a function of strain at room temperature. The bold (dashed) lines are related to infinite (finite-size, $L = 3\,\mu m$) silicene.

scattering, which couples nonequilibrium λ phonon modes to other phonon modes (λ', λ''). Detailed discussion on Δ_λ is given in [49,50]. Here, we employ the strain-dependent parameters to compute τ_λ. Setting Δ_λ to zero ($\tau_\lambda = \tau_\lambda^0$), yields the RTA phonon lifetime. Earlier study on thermal conductivity in strained silicene [39], has shown that RTA gives relatively good results that do not differ much from the fully iterative solution of the BTE. So we can treat the problem of scattering within the RTA.

It is well known that different scattering processes may contribute to the thermal conductivity. The phonon-phonon, phonon-boundary, phonon-isotope and phonon-vacancy scatterings are the main mechanisms for the phononic transport. Using Matthiessen's rule, τ_λ^0 can be obtained as [51,52]:

$$\frac{1}{\tau_\lambda^0} = \frac{1}{\tau_\lambda^{Ph}} + \frac{1}{\tau_\lambda^{B}} + \frac{1}{\tau_\lambda^{Iso}} + \frac{1}{\tau_\lambda^{V}}. \tag{4}$$

where τ_λ^{Ph}, τ_λ^{B}, τ_λ^{Iso} and τ_λ^{V} are the phonon–phonon [36], phonon-boundary [52–54], phonon-isotopic impurity [55–57] and phonon-vacancy [58] scattering lifetimes, respectively. In our previous study for unstrained silicene, we have described each one in detail [43]. In the case of non-zero strain, all above scattering lifetimes will change and result in new thermal conductivity values.

In order to keep this work reproducible, details of ab initio harmonic and anharmonic force constant calculations performed in Ref. [39] is given in Supplementary Information.

3. Results and discussion

We first calculate the effect of tensile strain on the total thermal conductivity and contributions from the distinct phonon branches of naturally occurring silicene (silicene structure with natural composition of silicon isotopes) in the absence of defects.

Increasing strain has two effects on the silicene structure. The Si-Si bond length increases with enhancing strain. On the other hand, the structure becomes more planar under larger strain. Increasing the Si-Si bond length will weaken the interatomic interactions in the in-plane direction. As a result of these effects, the group velocity of the phonons will undergo changes in different branches. These variations can modify the branches contributions to the thermal conductivity. However, the main reason for the change in silicene thermal conductivity with strain enhancement turns out to be the buckling reduction (the structure flattening). As the silicene structure flattens, the coupling of the in-plane and out-of-plane modes decreases. As a result of these changes, the scattering channels for phonons, specially out-of-plane modes are reduced. That gives rise to a significant increase in thermal conductivity. In Fig. 3, we display the room temperature total thermal conductivities of the infinite and finite-size ($L = 3\,\mu m$) silicene monolayers as functions of tensile strain computed within the RTA and compare contributions from different phonon branches. It can be seen that while the thermal conductivity of finite-size silicene increases with strain; for infinite sample, by strain enhancement, the thermal conductivity first increases to a maximum value, then decreases and finally reaches to an almost constant value. In the latter case, the maximum of the thermal conductivity appears at 4% strain, and its value is about one order of magnitude larger than that for the unstrained silicene. This size-dependent behavior can be understood from the changes of the distinct modes contributions to the thermal conductivity. As one can observe, while the contributions of optical modes to the thermal conductivity are mostly small and equivalent in both sample sizes, the LA and TA modes have dominant contributions when the strain is small and lead to a maximum value at 4% (3%) strain and then decrease (first decrease and again increase with a second peak at 8%) in the infinite (finite-size) silicene. Moreover, the thermal conductivity contributed by the ZA mode, first enhances with the strain up to 6%, then exhibits a reduction from 6% to 8% and again an increase from 8% to 10%. Since in infinite silicene, the important LA and TA contributions exhibit only one maximum and the mode-dependent variations are more pronounced, a peak in total thermal conductivity can be observed.

An important factor that significantly affects the thermal conductivity is temperature. The changes of lattice thermal conductivity with strain at different temperatures for finite-size ($L = 3\,\mu m$) and infinite silicene are illustrated in Figs. 4 and 5, respectively. As expected, with growing temperature, the thermal conductivity decreases but, interestingly, this reduction varies with strain and becomes larger beyond 2% strain. In addition, in the case of infinite silicene, the peak in thermal conductivity at 4% strain, gradually disappears by increasing the temperature. This can be explained by this fact that the size or boundary effect weakens at high temperatures, thus, the behavior of phononic thermal conductivities becomes less sensitive to the size and appears to be similar for both infinite and finite-size silicene. To support this discussion, one may notice that, the difference between the results of infinite and finite-size slicene is about 20 percent at high strain value (10%) at room temperature, while this is reduced by about 10 percent around $T = 600$ K. For a better understanding, we illustrate the variations of thermal conductivity with both strain and temperature for some different sizes of silicene ($L = 0.3$, 3, 30 μm and infinite) in Fig. 6 and show how the temperature rise governs the thermal conductivity of strained clean silicene.

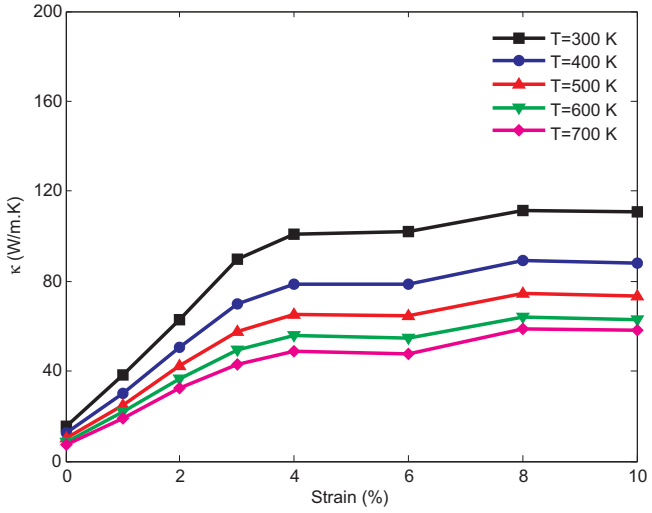

Fig. 4. Thermal conductivity of the finite-size ($L = 3\,\mu m$) clean silicene as a function of strain at different temperatures.

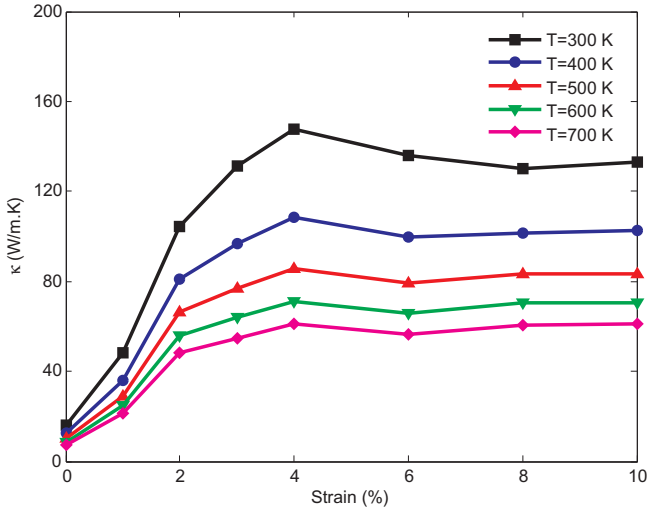

Fig. 5. Thermal conductivity of the infinite clean silicene as a function of strain at different temperatures.

As pointed out in Introduction, we are also interested to investigate the changes of the phononic thermal conductivities of strained silicene in the presence of important phonon-boundary and phonon-vacancy defect scattering mechanisms. First, we calculate the variations of thermal conductivity of a defectless silicene with strain at different specularity parameters to study the effect of phonon-boundary scattering. Fig. 7 shows the room temperature thermal conductivity of finite-size silicene ($L = 3\,\mu m$) as a function of strain for some typical specularity parameters, $P = 0$, 0.4, 0.8 and 1. It can be seen that by increasing the specularity parameter from zero to unity and changing the nature of boundary scattering from diffusive to specular, a peak in κ at 4% appears and grows gradually. This behavior can also be observed when the sample size is increased [39]. In the case of completely specular sample, $P = 1$, where the boundary scattering has no effect on the thermal conductivity, the result is exactly the same as for the infinite silicene. Also, it is visible that the effect of specularity parameter is more pronounced at intermediate strain values.

It is well known that the shape and location of vacancy defects have considerable effect on the thermal conductivity [47,59]. In our previous work [43], we studied the effect of a single vacancy defect (see Fig. 8) on the thermal conductivity of unstrained silicene. We assumed that these defects were uniformly distributed in the material and not

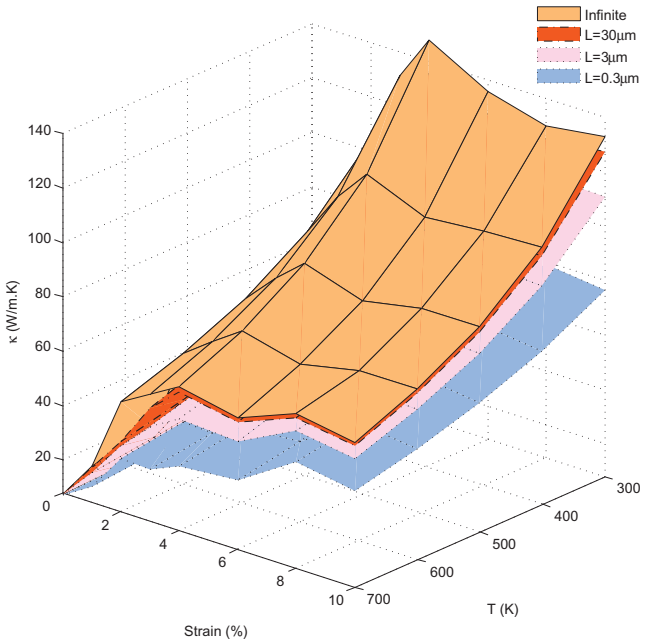

Fig. 6. Thermal conductivity of the finite-size clean silicene as a function of temperature and strain for some sample sizes.

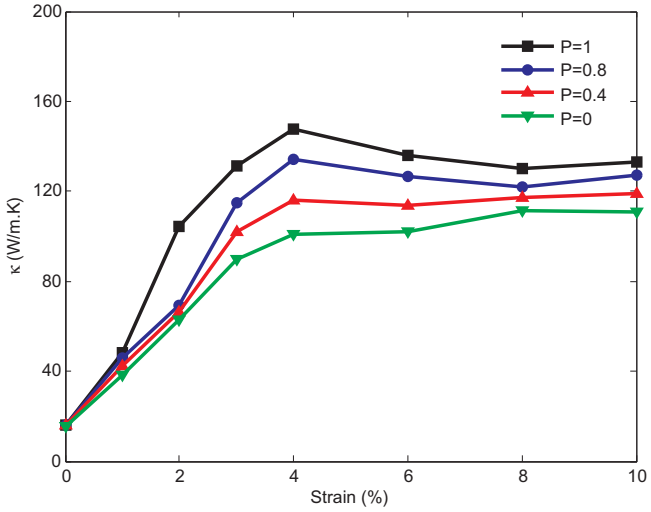

Fig. 7. The variations of thermal conductivity of the finite-size ($L = 3\,\mu m$) silicene with strain for some typical specularity parameters at $T = 300K$.

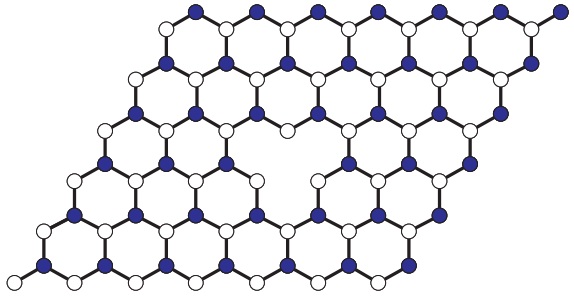

Fig. 8. Schematic description of silicene with a single vacancy defect.

accumulated in a particular sample location, such as the edges or only the center. To make the point clearer, if we had only one defect, it would be located at the sheet center. However, as the number of

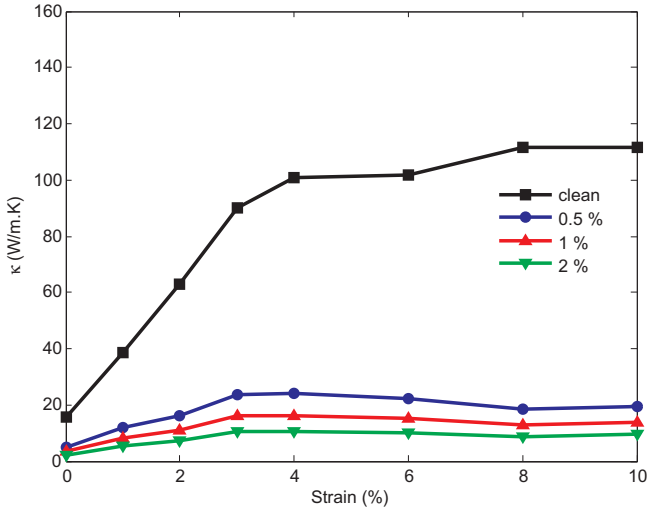

Fig. 9. The variation of thermal conductivity of the vacancy defected finite-size, $L = 3\,\mu m$, silicene with strain at room temperature. Here, the single vacancy concentration percentages are 0, 0.5, 1 and 2.

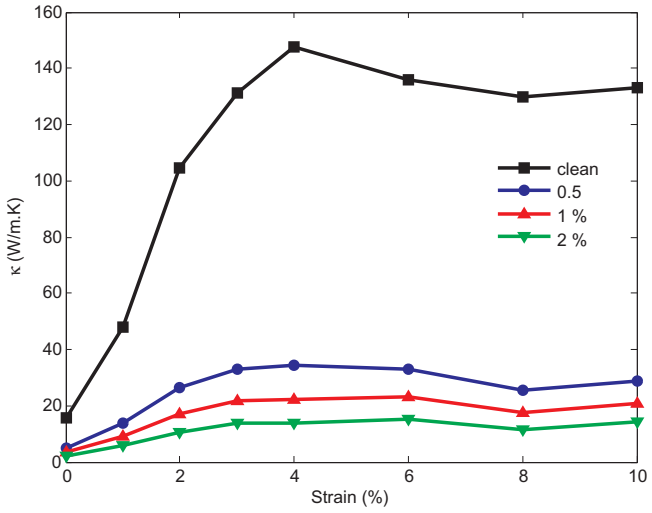

Fig. 10. The variation of thermal conductivity of the vacancy defected infinite silicene with strain at room temperature. Here, the single vacancy concentration percentages are 0, 0.5, 1 and 2.

vacancies increases, the missing silicon atoms are uniformly distributed throughout the sample. We found that the presence of single vacancy defects significantly decreases the thermal conductivity values in silicene. Our results showed that at the smallest single vacancy concentration studied there, 0.25 %, i.e. the case in which only one of the every 400 atoms of Si is removed, the reduction in the thermal conductivity is highly significant being about 42%. So, it is also interesting to investigate the impact of the single vacancy defects on the strained silicene in which the thermal conductivity has already much increased by the tensile strain. Figs. 9 and 10 demonstrate the changes of room temperature thermal conductivities as functions of strain at different single vacancy defect concentrations for finite-size ($L = 3\,\mu m$) and infinite silicene, respectively. In general, the reduction of thermal conductivity due to the vacancy defects not only apparently varies with strain magnitude but also is much stronger in silicene under strain. Our calculations show that the suppression of the thermal conductivity of strained silicene by the vacancy defects is quite remarkable in such a way that removing one of every 100 Si atoms (1% vacancy concentration) leads to a substantial reduction of about 87% in thermal conductivity at 8% strain while it has a maximum value of 75% in

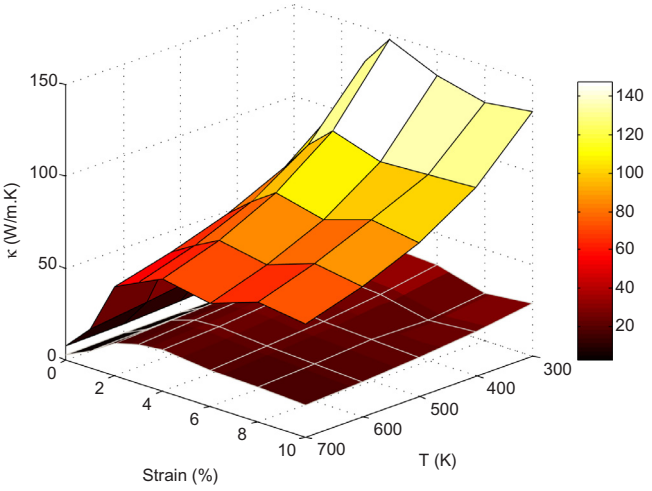

Fig. 11. Thermal conductivity of the silicene as a function of strain and temperature. The lower (upper) surface belongs to the vacancy defected (clean) infinite silicene. Here, the single vacancy concentration is set to 1%.

unstrained silicene. Also, as Fig. 9 displays, contrary to the monotonically increase of κ in clean finite-size ($L = 3\,\mu m$) silicene, thermal conductivity of vacancy-defected silicene first increases and then slowly decreases with strain.

In addition, compared to the finite-size silicene, the infinite strained sample is even more affected by the vacancy defects. A noteworthy point, as observed in Fig. 10, is that by increasing the vacancy defect concentration, the peak of thermal conductivity at 4% strain, first vanishes and then reappears at a higher strain value, *i. e.* 6% strain. This behavior is a consequence of the competition between two opposite effects; while the increase of the strain, first brings about an enhancement and then a slow reduction, the phonon-vacancy defect scattering always has a decreasing effect on the thermal conductivity. So, considering a small amount of vacancy defect centers which usually found in real crystals, can completely remove the previously predicted peak from the κ curve in infinite silicene. To complete the discussion, we demonstrate the phononic thermal conductivity changes of vacancy-defected (clean) infinite silicene with both the strain and temperature in lower (upper) surface of Fig. 11. According to this figure, with rising the temperature and as a result, intensifying the phonon–phonon scattering, the difference between the clean and defected silicene reduces for all strain values. At high temperatures, the vacancy-defect scattering still plays an important role but the calculated thermal conductivity becomes less sensitive to the strain. While high lattice thermal conductivity is useful in some applications such as electronic cooling, in thermoelectric devices materials with low thermal conductivity, like silicene, is required. By adjusting these system parameters, we can probably achieve the desired conditions.

4. Conclusions

In summary, we have theoretically studied the behavior of thermal conductivity of strained silicene in the presence of important scattering mechanisms. Based on a solution to the linearized phonon BTE within the RTA, we calculate the separate and combined effects of temperature, specularity parameter and defects on the thermal conductivity of silicene under an uniform biaxial tensile strain. We compare our results for infinite and finite-size samples. These calculations are intended to describe how the strain-induced variation of the thermal conductivity is affected by temperature, boundary scattering and single-vacancy defects. Our results have demonstrated that by rising temperature, the effect of strain gradually weakens and even the peak at 4% strain is clearly diminished in infinite silicene. In addition, the behaviors of thermal conductivity of infinite and finite-size strained silicene become

similar at higher temperatures and almost strain independent at large values of strain. Moreover, it was found that the influence of the specularity parameter is noticeable at intermediate strain values. On the other hand, our calculations have shown that the suppression of thermal conductivity by the vacancy defects is quite remarkable and much stronger in strained silicene in such a way that, by removing one of every 100 Si atoms (1% vacancy concentration) a maximum reduction of about 87% in thermal conductivity of silicene sample at 8% strain is achievable at room temperature. Also, the increasing behavior of finite-size silicene thermal conductivity with strain is affected by the single-vacancy defects. Finally, we have shown that at larger vacancy concentrations, the peak of thermal conductivity is shifted towards higher strains, in an infinite sample. Considering important scattering mechanisms and a detailed analysis on system parameters have enabled us to present a more complete picture of the thermal conductivity in silicene, which can probably be useful in phononic engineering and nanotechnology.

CRediT authorship contribution statement

M. Barati: Conceptualization, Software, Writing - original draft. **T. Vazifehshenas:** Supervision, Conceptualization, Writing - review & editing. **T. Salavati-fard:** Validation, Writing - review & editing. **M. Farmanbar:** Validation, Writing - review & editing.

Declaration of Competing Interest

The authors declare that they have no known competing financial interests or personal relationships that could have appeared to influence the work reported in this paper.

Acknowledgments

We would like to thank D.r Han Xie for sharing with us the second and third-order force constants of strained silicene. The support and resources from the Center for High Performance Computing at Shahid Beheshti University of Iran are gratefully acknowledged.

Appendix A. Supplementary data

Supplementary data associated with this article can be found, in the online version, athttps://doi.org/10.1016/j.commatsci.2019.109407.

References

[1] A.K. Geim, K.S. Novoselov, Nature Mater. 6 (2007) 183.
[2] K.S. Novoselov, A.K. Geim, S.V. Morozov, D. Jiang, Y. Zhang, S.V. Dubonos, I.V. Grigorieva, A.A. Firsov, Science 306 (2004) 666.
[3] S. Cahangirov, M. Topsakal, E. Akturk, H. Sahin, S. Ciraci, Phys. Rev. Lett. 102 (2009) 236804 .
[4] S. Javadian, S.M. Atashzar, H. Gharibi, M. Vafaee, Comput. Mater. Sci 165 (2019) 144–153.
[5] P. De Padova, P. Perfetti, B. Olivieri, C. Quaresima, C. Ottaviani, G. Le Lay, J. Phys.: Condens. Matter 24 (2012) 223001 .
[6] J. Klinovaja, D. Loss, Phys. Rev. B 88 (2013) 075404 .
[7] A. Sannyal, Y. Ahn, J. Jang, Comput. Mater. Sci 165 (2019) 121–128.
[8] J.D. Renteria, D.L. Nika, A.A. Balandin, Appl. Sci. 4 (2014) 525.
[9] L. Tao, E. Cinquanta, D. Chiappe, C. Grazianetti, M. Fanciulli, M. Dubey, A. Molle, D. Akinwande, Nat. Nanotechnol. 10 (2015) 227.
[10] A.C. Ferrari, F. Bonaccorso, V. Fal'Ko, K.S. Novoselov, S. Roche, P. Bggild, S. Borini, F.H. Koppens, V. Palermo, N. Pugno, et al., Nanoscale 7 (2015) 4598.
[11] M. Mirzaei, T. Vazifehshenas, T. Salavati-fard, M. Farmanbar, B. Tanatar, Phys. Rev. B 98 (2018) 045429 .
[12] J. Wu, H. Wen, H. Shi, C. Chen, B. Huang, Y. Wei, M. Li, Superlattices Microstruct. 130 (2019) 258–266.
[13] D. Zha, C. Chen, J. Wu, Solid State Commun. 219 (2015) 21–24.
[14] M. Houssa, A. Dimoulas, A. Molle, J. Phys. Condence. Matter 27 (2015) 253002 .
[15] J. Zhao, H. Liu, Z. Yu, R. Quhe, S. Zhao, Y. Wang, C.C. Liu, H. Zhang, N. Han, Y. Yan, K. Wu, Progress Mater. Sci. 83 (2016) 24–151.
[16] R.E. Roman, S.W. Cranford, Comput. Mater. Sci 82 (2014) 50–55.
[17] C. Liu, W. Feng, Y. Yao, Phys. Rev. Lett. 107 (2011) 076802 .
[18] C. Liu, H. Jiang, Y. Yao, Phys. Rev. B 84 (2011) 195430 .
[19] X. Zhai, G. Jin, J. Phys.: Condens. Matter 28 (2016) 355002 .
[20] N. Dadkhah, T. Vazifehshenas, M. Farmanbar, T. Salavati-fard, J. Appl. Phys. 125 (2019) 104302 .
[21] G. Liu, M.S. Wu, C.Y. Ouyang, B. Xu, EPL 125 (2012) 17010.
[22] G.G. Guzmn-Verri, L.C. Lew, Yan Voon, Phys. Rev. B 99 (2007) 075131 .
[23] H. Sahin, S. Cahangirov, M. Topsakal, E. Bekaroglu, E. Akturk, R.T. Senger, S. Ciraci, Phys. Rev. B 80 (2009) 155453 .
[24] B. Aufray, A. Kara, S. Vizzini, H. Oughaddou, C. Leandri, B. Ealet, G. Le Lay, Appl. Phys. Lett. 96 (2010) 183102 .
[25] P. De Padova, C. Quaresima, B. Olivieri, P. Perfetti, G. Le Lay, Appl. Phys. Lett. 98 (2011) 081909 .
[26] A. Kara, H. Enriquez, A.P. Seitsonen, L.C.L.Y. Voon, S. Vizzini, B. Aufray, H. Oughaddou, Surf. Sci. Rep. 67 (2012) 1–18.
[27] S.M. Aghaei, I. Torres, I. Calizo, Comput. Mater. Sci 138 (2017) 204–212.
[28] N.D. Drummond, V. Zolyomi, V.I. Fal'ko, Phys. Rev. B 85 (2012) 075423 .
[29] Z.Y. Ni, Q.H. Liu, K.C. Tang, J.X. Zheng, J. Zhou, R. Qin, Z.X. Gao, D.P. Yu, J. Lu, Nano Lett. 12 (2012) 113–118.
[30] B.J. Feng, Z.J. Ding, S. Meng, Y.G. Yao, X.Y. He, P. Cheng, L. Chen, K.H. Wu, Nano Lett. 12 (2012) 3507–3511.
[31] P. Vogt, P. De Padova, C. Quaresima, J. Avila, E. Frantzeskakis, M.C. Asensio, A. Resta, B. Ealet, G. Le Lay, Phys. Rev. Lett. 108 (2012) 155501 .
[32] B. Bishnoi, B. Ghosh, Comput. Mater. Sci 85 (2014) 16–19.
[33] T.P. Kaloni, Y.C. Cheng, U. Schwingenschlogl, J. Appl. Phys. 113 (2013) 104305 .
[34] Z. Yan, D.L. Nika, A.A. Balandin, I.E.T. Circuits, Devices and Systems. 9 (2015) 4–12.
[35] A.A. Balandin, ECS Trans. 67 (1) (2015) 167.
[36] X. Gu, R. Yang, J. Appl. Phys. 117 (2015) 025102 .
[37] X. Zhang, H. Xie, M. Hu, H. Bao, S. Yue, G. Qin, G. Su, Phys. Rev. B 89 (2014) 054310 .
[38] B. Peng, H. Zhang, Y. Xu, G. Ni, R. Zhang, H. Zhu, Phys. Rev. B 94 (2016) 245420 .
[39] H. Xie, T. Ouyang, E. Germaneau, G. Qin, M. Hu, H. Bao, Phys. Rev. B 93 (2016) 075404 .
[40] Y.D. Kuang, L. Lindsay, S.Q. Shi, G.P. Zheng, Nanoscale 8 (2016) 3760.
[41] Z. Wang, T. Feng, X. Ruan, J. Appl. Phys. 117 (2015) 084317 .
[42] X. Zhang, H. Bao, M. Hu, Nanoscale 7 (2015) 6014.
[43] M. Barati, T. Vazifehshenas, T. Salavati-fard, M. Farmanbar, J. Phys.: Condens. Matter. 30 (2018) 155307 .
[44] M. Spencer, T. Morishita, Silicene: Structure, Properties and Applications, Springer, 2016.
[45] Q.X. Pei, Y.W. Zhang, Z.D. Sha, V.B. Shenoy, J. Appl. Phys. 114 (2013) 033526 .
[46] B. Liu, C.D. Reddy, J. Jiang, H. Zhu, J.A. Baimova, S.V. Dmitriev, K. Zhou, J. Phys. D: Appl. Phys. 47 (2014) 165301 .
[47] H.P. Li, R.Q. Zhang, EPL 99 (2012) 36001.
[48] M. Hu, X. Zhang, D. Poulikakos, Phys. Rev. B 87 (2013) 195417 .
[49] L. Lindsay, D.A. Broido, Phys. Rev. B 85 (2012) 035436 .
[50] W. Li, L. Lindsay, D.A. Broido, D.A. Stewart, N. Mingo, Phys. Rev. B 86 (2012) 174307 .
[51] G.P. Srivastava, The Physics of Phonons, Adam Hilger, Bristol, 1990.
[52] W. Li, J. Carrete, N. Mingo, Appl. Phys. Lett 103 (2013) 253103 .
[53] J.M. Ziman, Electrons and Phonons, Clarendon Press, London, 1960.
[54] D.L. Nika, E.P. Pokatilov, A.S. Askerov, A.A. Balandin, Phys. Rev. B 79 (2009) 155413 .
[55] L. Lindsay, D.A. Broido, T.L. Reinecke, Phys. Rev. Lett. 109 (2012) 095901 .
[56] S.I. Tamura, Phys. Rev. B 27 (1983) 858.
[57] L. Lindsay, D.A. Broido, Phys. Rev. B 85 (2012) 035436 .
[58] G. Xie, Y. Shen, X. Wei, L. Yang, H. Xiao, J. Zhong, G. Zhang, Sci. Rep. 4 (2014) 5085.
[59] J.W. Jiang, B.S. Wang, J.S. Wang, Appl. Phys. Lett. 98 (2011) 113114.